# Supporting Information

# Sucrose-derived hard carbon wrapped by reduced graphene oxide for high-performance anode of sodium-ion batteries

*Shengyuan Li,[1] Hong Yuan,[1] Chuanren Ye,[1] Yizhe Wang,[1] Long Wang,[2] Kun Ni,[1,*] and Yanwu Zhu,[1,3,*]*

[1] *Department of Materials Science and Engineering, School of Chemistry and Materials Science, University of Science and Technology of China, Hefei, Anhui 230026, P. R. China*

[2] *Fu'an Guolong Nano Material, Co. Ltd, Ningde, Fujian 352000, P. R. China*

[3] *Hefei National Research Center for Physical Sciences at the Microscale, University of Science and Technology of China, Hefei, Anhui 230026, P. R. China*

*Corresponding Authors: zhuyanwu@ustc.edu.cn (Y. Zhu); nikun@ustc.edu.cn (K. Ni)

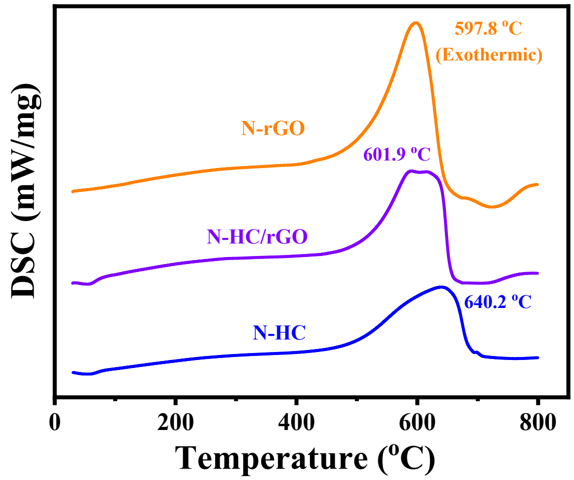


Figure S1. DSC results of N-HC, N-rGO and N-HC/rGO.

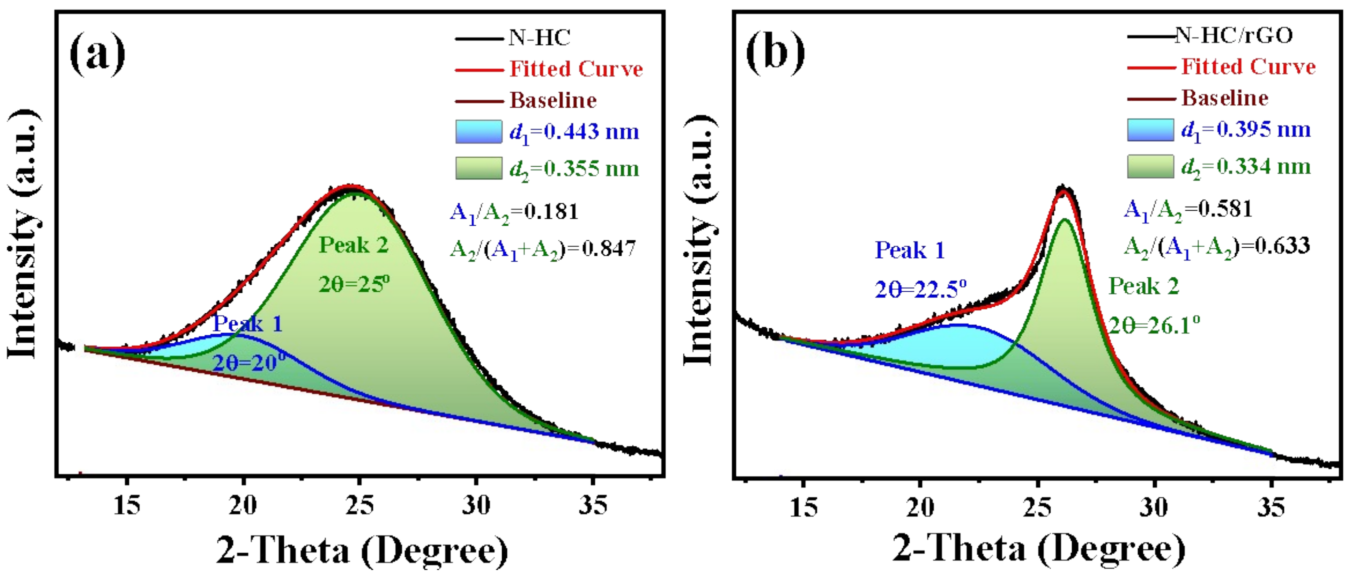


Figure S2. Fitting of XRD (002) peak of (a) N-HC and (b) N-HC/rGO.

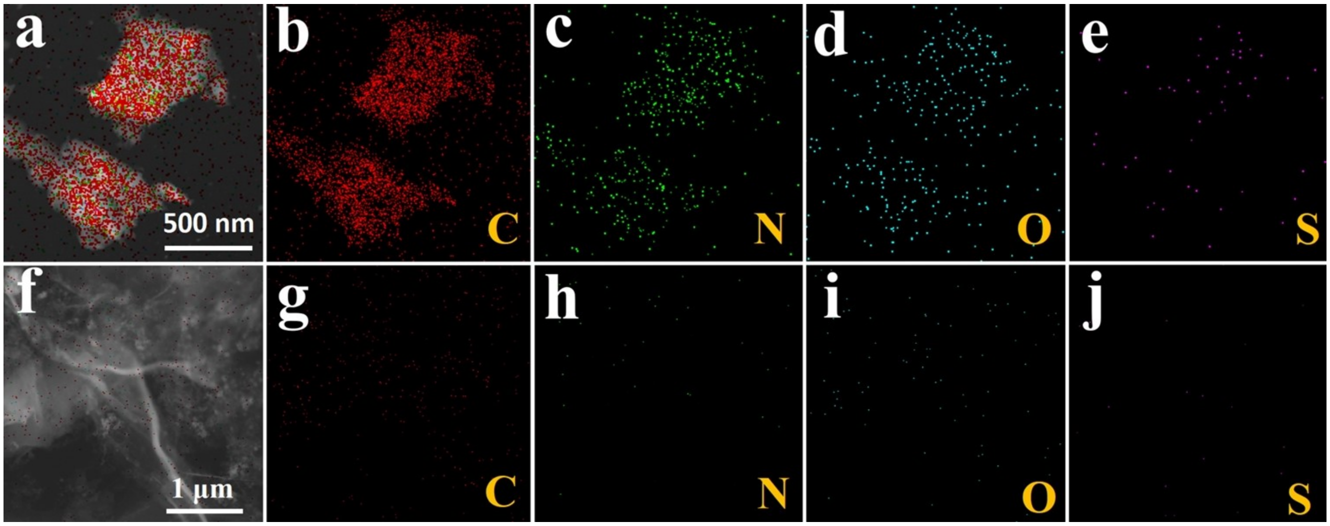


Figure S3. EDS elemental mappings of (a–e) N-HC and (f–j) N-HC/rGO.

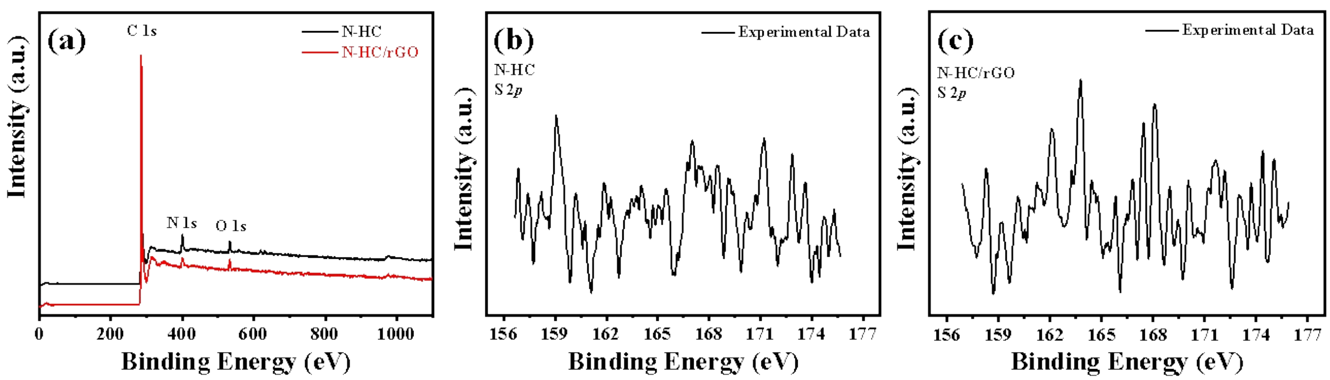


Figure S4. (a) XPS survey spectra of N-HC and N-HC/rGO. XPS spectra of S 2*p* of (b) N-HC and (c) N-HC/rGO.

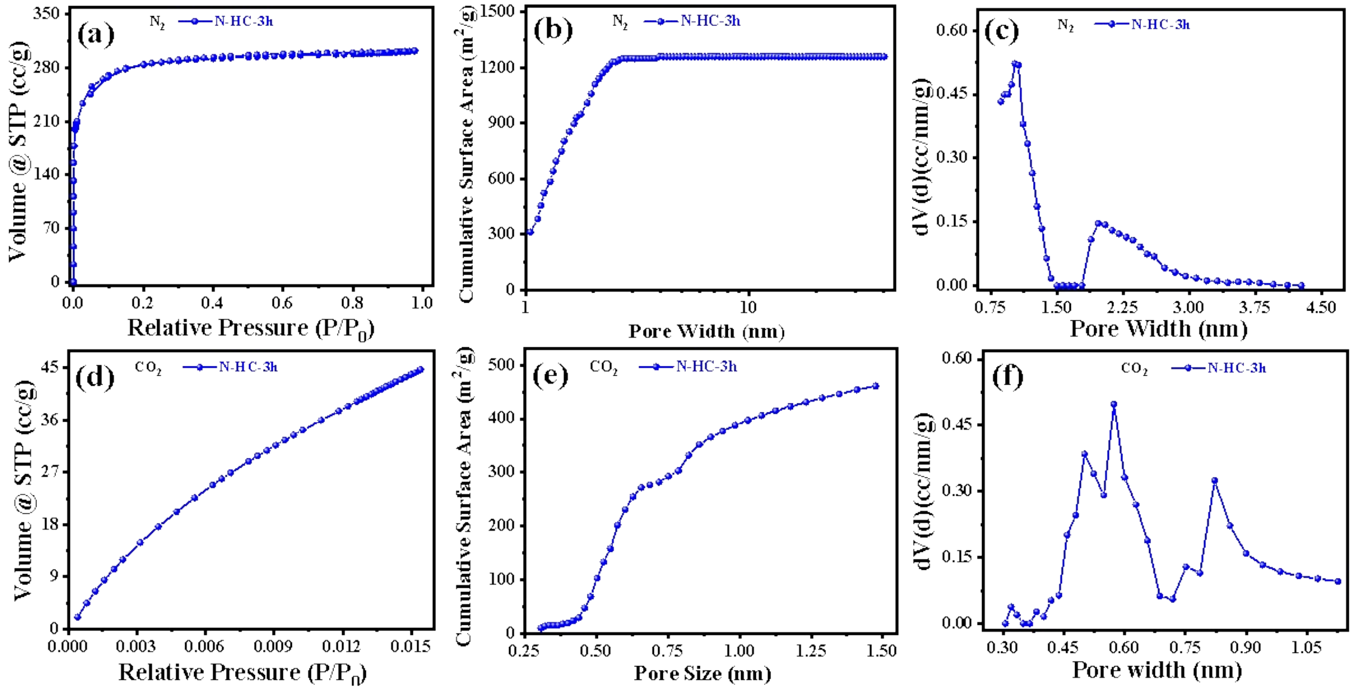


Figure S5. (a) $N_2$ adsorption/desorption and (d) $CO_2$ adsorption measurements of N-HC-3h sample; SSA and pore size distribution determined by NLDFT calculation of (b) $N_2$ adsorption/desorption and (e) $CO_2$ adsorption measurements; Pore size distribution determined by NLDFT calculation for (c) $N_2$ adsorption/desorption and (f) $CO_2$ adsorption measurements.

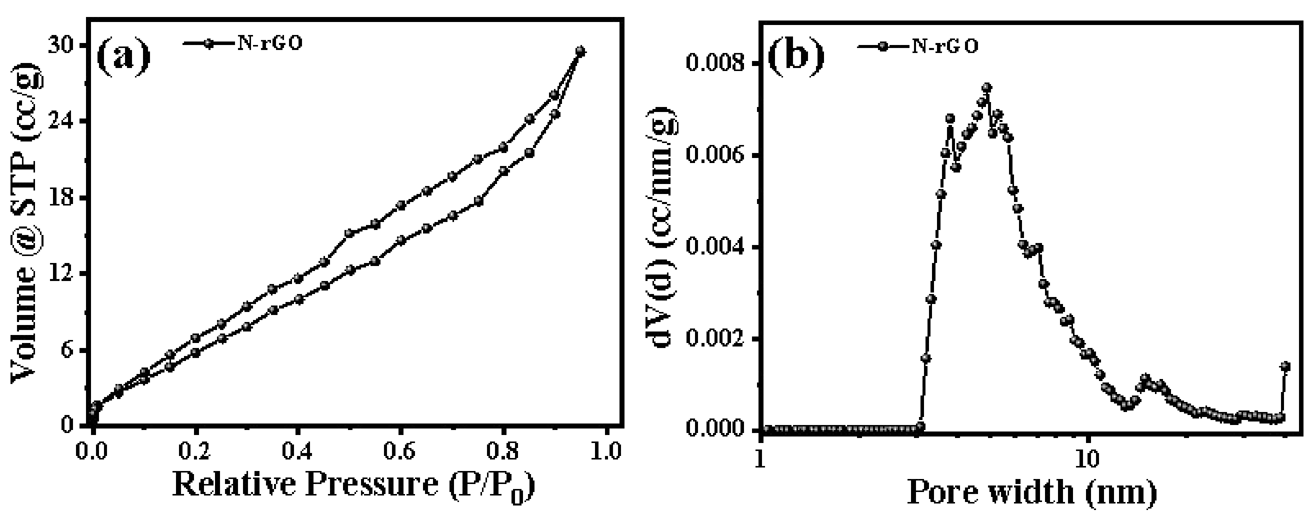


Figure S6. (a) $N_2$ adsorption/desorption and (b) corresponding pore size distribution by NLDFT calculation of N-rGO.

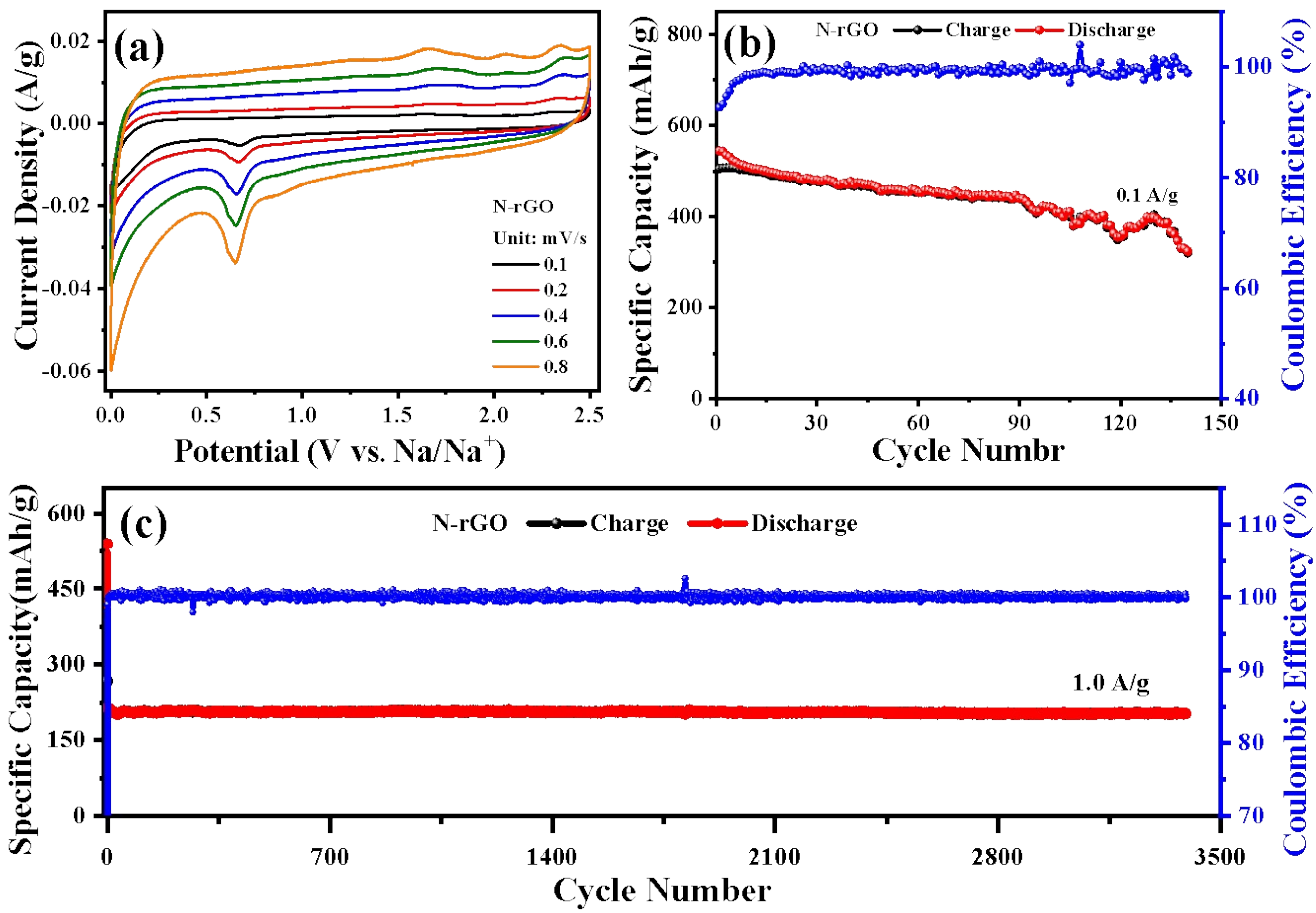


Figure S7. Electrochemical performance of N-rGO electrode. (a) CV curves at different scan rates; Cycling test of N-rGO electrode at (b) 0.1 and (c) 1.0 A $g^{-1}$.

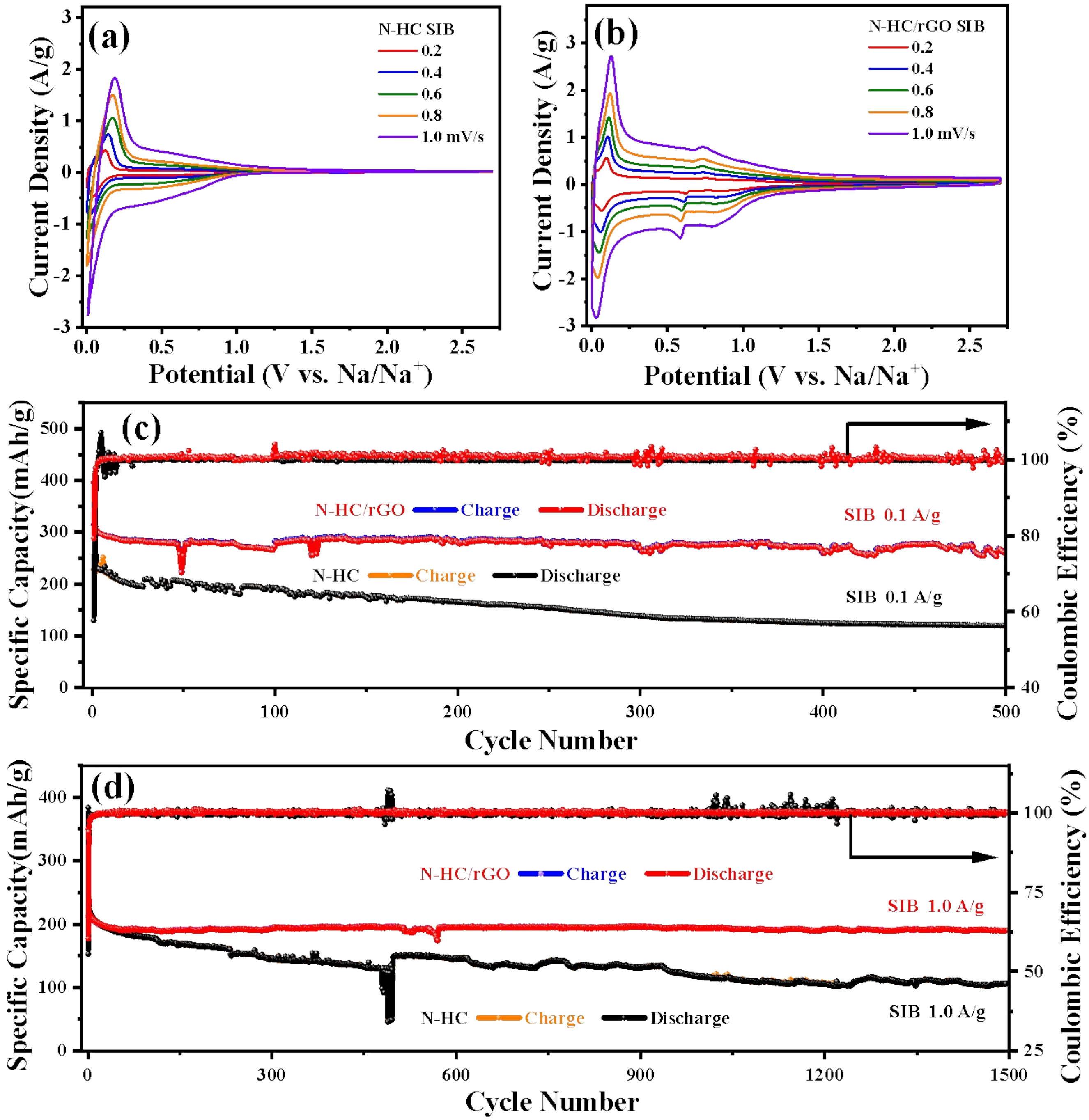


Figure S8. CV curves of (a) N-HC and (b) N-HC/rGO; Cycling test at (c) 0.1 A $g^{-1}$ and (d) 1.0 A $g^{-1}$ of N-HC and N-HC/rGO, respectively.

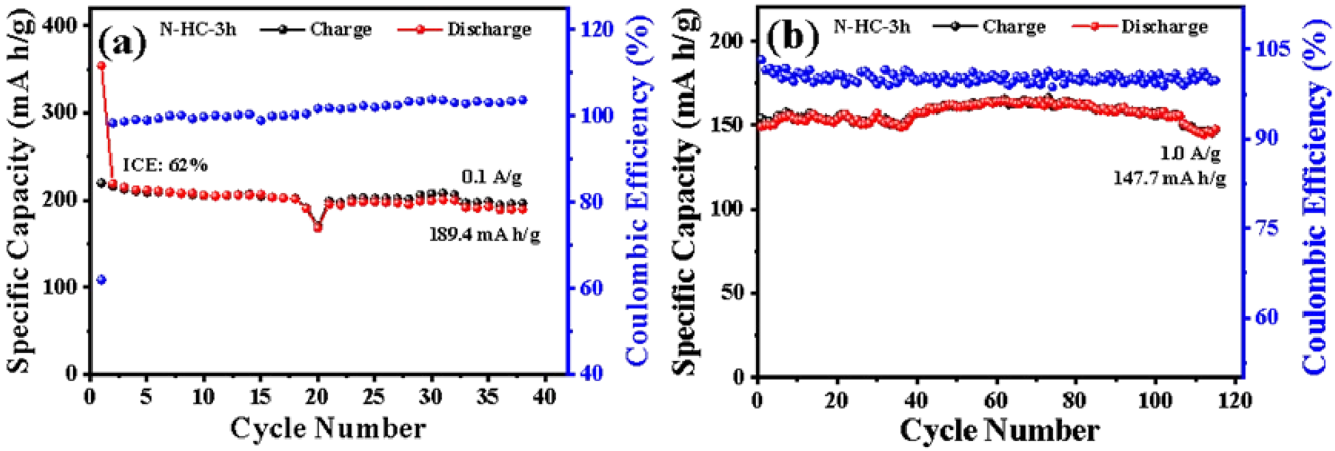


Figure S9. Cycling performance of N-HC-3h electrode at (a) 0.1 and (b) 1.0 A $g^{-1}$.

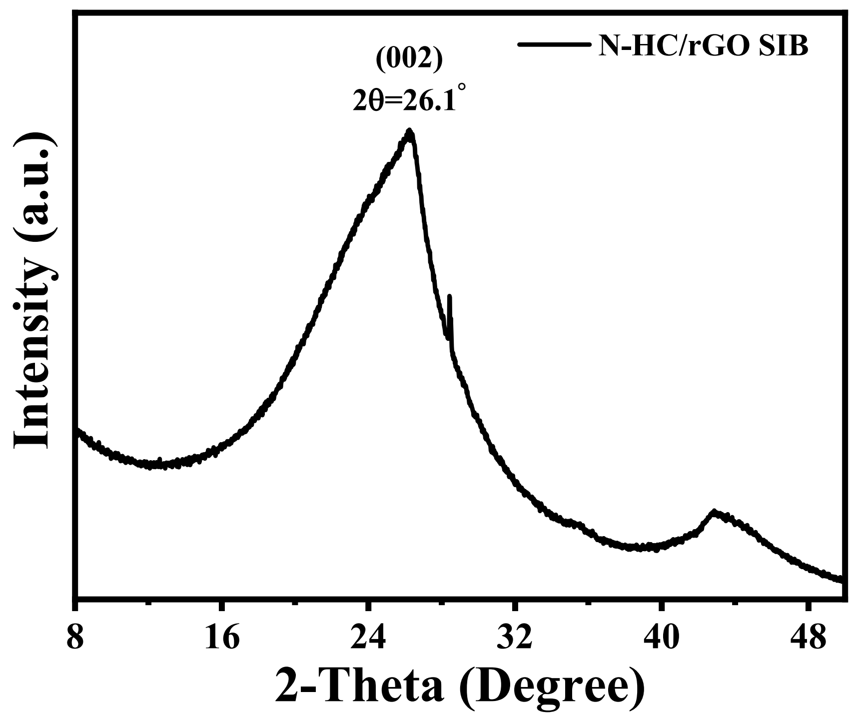


Figure S10. In-situ XRD result of N-HC/rGO electrode when discharged at 0.1 A $g^{-1}$.

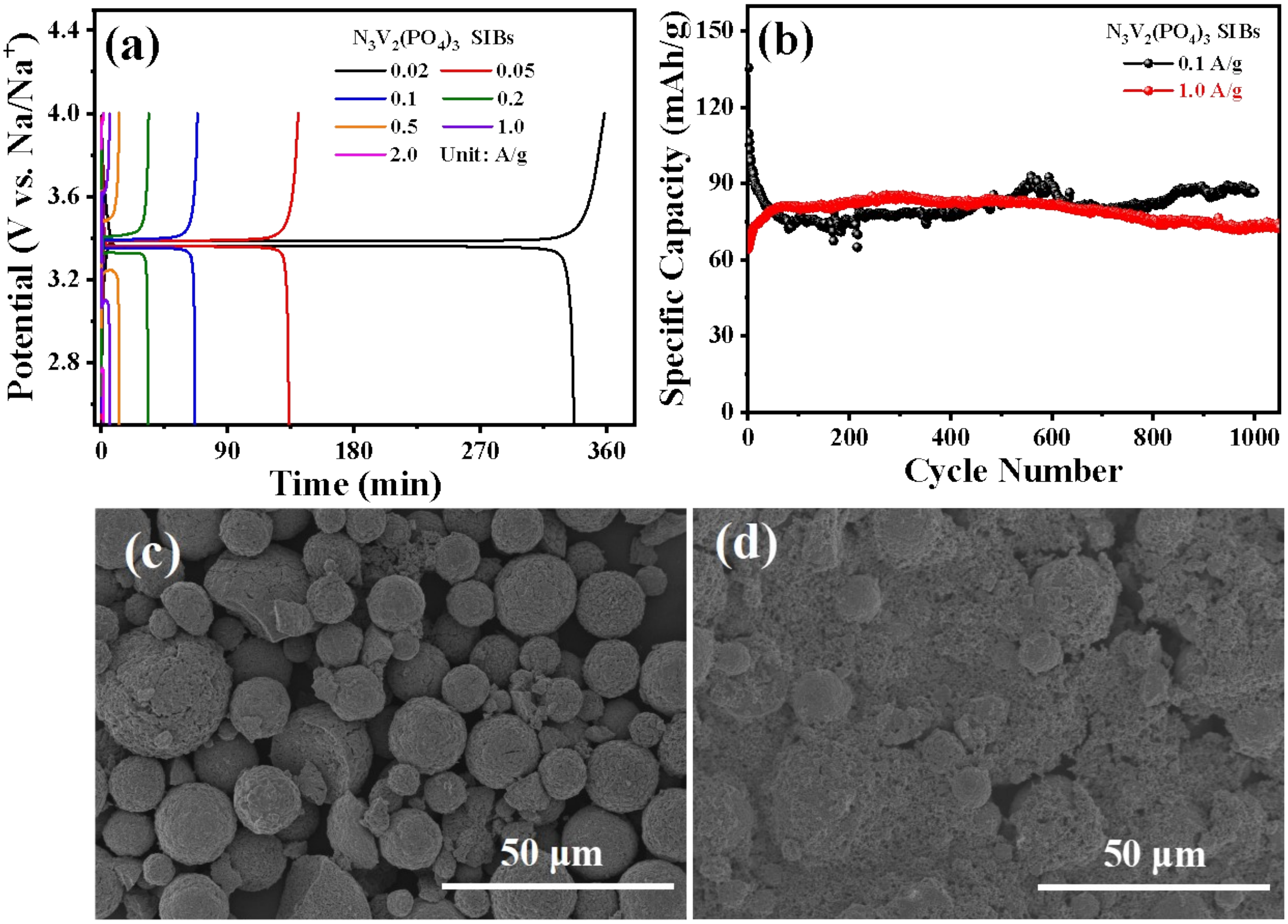


Figure S11. Electrochemical performance of NVP electrode. (a) Rate capability at various current densities from 0.02 to 2.0 A $g^{-1}$; (b) Cycling performances at 0.1 and 1.0 A $g^{-1}$; SEM images of NVP (c) before cycling and (d) after cycling at 0.1 A $g^{-1}$ after 50 cycles.

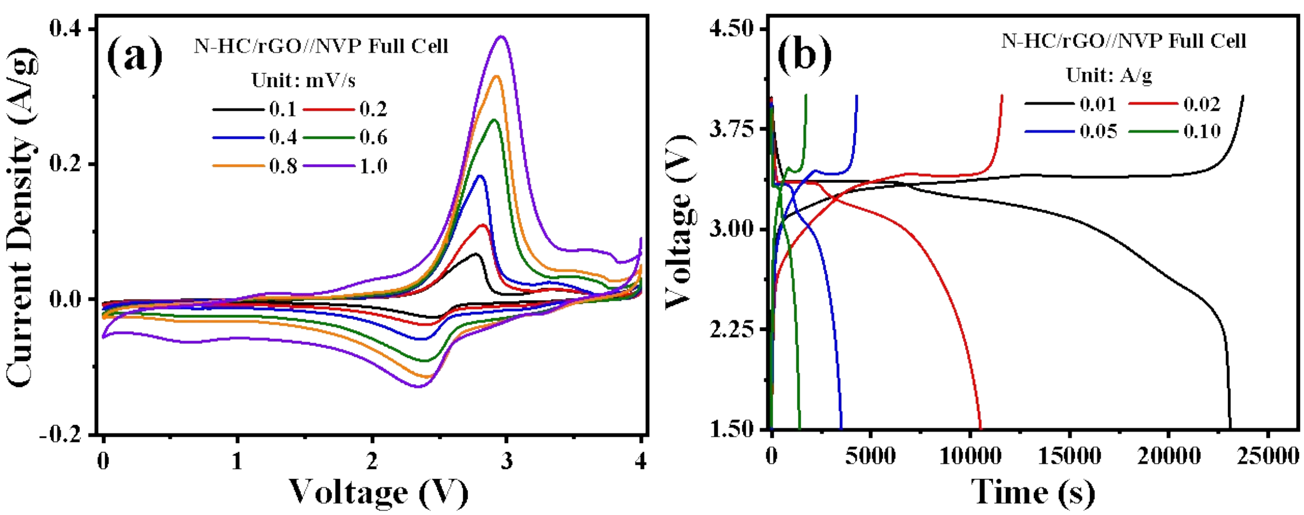


Figure S12. Electrochemical performance of N-HC/rGO//NVP full cell. (a) CV curves at various sweep rates from 0.1 to 1.0 mV $s^{-1}$; (b) Rate capability at various current densities from 0.01 to 0.1 A $g^{-1}$.

Table S1. XPS data of N-HC and N-HC/rGO samples.

| | | N-HC | N-HC/rGO |
|---|---|---|---|
| C | C–C | 34.0% | 40.8% |
| | C=C | 35.8% | 22.4% |
| | C–N | 17.7% | 24.0% |
| | C–O | 7.4% | 6.3% |
| | C=O | 5.1% | 6.5% |
| N | Pyridinic–N | 28.7% | 41.5% |
| | Pyrrolic–N | 43.5% | 42.2% |
| | Quaternary–N | 27.8% | 16.3% |
| O | O=C | 30.1% | 38.6% |
| | O–C | 51.4% | 50.7% |
| | O=C–OH | 18.5% | 10.7% |
| C (Atomic %) | | 89.32% | 93.28% |
| N (Atomic %) | | 7.94% | 4.15% |
| O (Atomic %) | | 2.73% | 2.58% |

Table S2. Comparison with the hard carbon electrodes in the previous works.

| Materials | Electrolytes | Rate Capability | Cycle performance and Capacity retain | ICE [%] | Ref. |
|---|---|---|---|---|---|
| **N-HC/rGO** | 1 M $NaPF_6$ in DEGDME | 355.5 mA h $g^{-1}$ at 50 mA $g^{-1}$; 321.9 mA h $g^{-1}$ at 100 mA $g^{-1}$; 266.8 mA h $g^{-1}$ at 1000 mA $g^{-1}$; | 407.3 mA h $g^{-1}$ after 100 cycles at 10 mA $g^{-1}$, ~78.7%; 261.4 mA h $g^{-1}$ after 500 cycles at 100 mA $g^{-1}$, ~84%; 190.5 mA h $g^{-1}$ after 1500 cycles at 1000 mA $g^{-1}$, ~80.7%; | 84.7 | This work |
| **N-HC** | | 284 mA h $g^{-1}$ at 50 mA $g^{-1}$; 273.9 mA h $g^{-1}$ at 100 mA $g^{-1}$; 157.4 mA h $g^{-1}$ at 1000 mA $g^{-1}$; | 199.1 mA h $g^{-1}$ after 100 cycles at 10 mA $g^{-1}$, ~56.7%; 120.2 mA h $g^{-1}$ after 500 cycles at 100 mA $g^{-1}$, ~51.2%; 105.8 mA h $g^{-1}$ after 1500 cycles at 1000 mA $g^{-1}$, ~47.9%; | 75.1 | |
| Corn cob derived HC | 0.6 M $NaPF_6$ in EC/DEC | 360 mA h $g^{-1}$ at 30 mA $g^{-1}$1; 288 mA h $g^{-1}$ at 150 mA $g^{-1}$; 211 mA h $g^{-1}$ at 600mA $g^{-1}$; | 275 mA h $g^{-1}$ after 100 cycles at 60 mA $g^{-1}$, ~97% | 86 | [1] |
| Shaddock peel derived HC | 1 M $NaClO_4$ in EC/DEC | 430.5 mA h $g^{-1}$ at 30 mA $g^{-1}$; 373.5 mA h $g^{-1}$ at 50 mA $g^{-1}$; 317.7 mA h $g^{-1}$ at 100 mA $g^{-1}$; | 352 mA h $g^{-1}$ after 200 cycles at 50 mA $g^{-1}$, ~97.5% | 67.7 | [2] |
| Lotus seedpod derived HC | 1 M $NaClO_4$ in PC with 2% FEC | 330.6 mA h $g^{-1}$ at 50 mA $g^{-1}$; 288.9 mA h $g^{-1}$ at 100 mA $g^{-1}$; 78.3 mA h $g^{-1}$ at 1000 mA $g^{-1}$; | 295 mA h $g^{-1}$ after 200 cycles at 50 mA $g^{-1}$, ~89.7%; 161.5 mA h $g^{-1}$ after 500 cycles at 200 mA $g^{-1}$, ~80%; | 50.4 | [3] |
| Wood fiber derived HC | 1 M $NaClO_4$ in EC/DEC | 260 mA h $g^{-1}$ at 100 mA $g^{-1}$; | 196 mA h $g^{-1}$ after 200 cycles at 100 mA $g^{-1}$, ~100%; | 72 | [4] |
| N-doped PVP derived HC | 1 M $NaClO_4$ in PC | 304 mA h $g^{-1}$ at 20 mA $g^{-1}$; 209 mA h $g^{-1}$ at 100 mA $g^{-1}$; 70 mA h $g^{-1}$ at 1000 mA $g^{-1}$; | 255 mA h $g^{-1}$ after 100 cycles at 20 mA $g^{-1}$, ~94%; | 47.7 | [5] |
| S-doped mesophase pitch derived HC | 1 M $NaClO_4$ in EC/DEC | 420 mA h $g^{-1}$ at 50 mA $g^{-1}$; 340 mA h $g^{-1}$ at 100 mA $g^{-1}$; 217 mA h $g^{-1}$ at 1000 mA $g^{-1}$; | 320 mA h $g^{-1}$ after 100 cycles at 100 mA $g^{-1}$; 200 mA h $g^{-1}$ after 1000 cycles at 4000 mA $g^{-1}$, ~100%; | 56 | [6] |
| P-doped sucrose derived HC | 1 M $NaPF_6$ in EC/DEC | 359 mA h $g^{-1}$ at 20 mA $g^{-1}$; ~250 mA h $g^{-1}$ at 100 mA $g^{-1}$; ~60 mA h $g^{-1}$ at 1000 mA $g^{-1}$; | 200 mA h $g^{-1}$ after 150 cycles at 40 mA $g^{-1}$, ~85%; | 73 | [7] |
| P-doped PVP derived HC | 1 M $NaClO_4$ in EC/DEC with 2% FEC | 384.5 mA h $g^{-1}$ at 20 mA $g^{-1}$; 320.1 mA h $g^{-1}$ at 100 mA $g^{-1}$; 134.6 mA h $g^{-1}$ at 1000 mA $g^{-1}$; | 386.4 mA h $g^{-1}$ after 100 cycles at 20 mA $g^{-1}$, ~98.2%; | 45 | [8] |
| Chitosan derived HC | 1 M $NaPF_6$ in DME | 275.4 mA h $g^{-1}$ at 50 mA $g^{-1}$; 206 mA h $g^{-1}$ at 2000 mA $g^{-1}$; 139 mA h $g^{-1}$ at 10000 mA $g^{-1}$1; | ~250 mA h $g^{-1}$ after 300 cycles at 50 mA $g^{-1}$; 196 mA h $g^{-1}$ after 2000 cycles at 1000 mA $g^{-1}$, ~90%; | 85.9 | [9] |
| Loofah sponge derived HC | 1 M $NaCF_3SO_3$ in DEGDME | 320 mA h $g^{-1}$ at 30 mA $g^{-1}$; 217 mA h $g^{-1}$ at 900 mA $g^{-1}$; 210 mA h $g^{-1}$ at 1500 mA $g^{-1}$; | 250 mA h $g^{-1}$ after 100 cycles at 150 mA $g^{-1}$, ~93%; | 63 | [10] |

| | | | | | |
|---|---|---|---|---|---|
| Cotton derived HC | 0.8 M $NaPF_6$ in EC/DEC | 315 mA h $g^{-1}$ at 30 mA $g^{-1}$; 275 mA h $g^{-1}$ at 150 mA $g^{-1}$; 180 mA h $g^{-1}$ at 300 mA $g^{-1}$; | 305 mA h $g^{-1}$ after 100 cycles at 30 mA $g^{-1}$, ~97%; | 83 | [11] |
| Pomelo peels | 1 m $NaClO_4$ in EC/PC | 278.8 mA h $g^{-1}$ at 50 mA $g^{-1}$; 207.8 mA h $g^{-1}$ at 100 mA $g^{-1}$; 118.4 mA h $g^{-1}$ at 1000 mA $g^{-1}$; 71 mA h $g^{-1}$ at 5000 mA $g^{-1}$; | 181 mA h $g^{-1}$ after 220 cycles at 200 mA $g^{-1}$, ~84.6%; | 27 | [12] |
| Sucrose | 1 M $NaClO_4$ in EC/DEC | 300 mA h $g^{-1}$ at 30 mA $g^{-1}$; 240 mA h $g^{-1}$ at 60 mA $g^{-1}$; 100 mA h $g^{-1}$ at 150 mA $g^{-1}$; | 222 mA h $g^{-1}$ after 100 cycles at 30 mA $g^{-1}$, ~80%; | 83 | [13] |
| Sucrose/GO | 1 M $NaClO_4$ in EC/DEC | 200 mA h $g^{-1}$ at 40 mA $g^{-1}$; 150 mA h $g^{-1}$ at 100 mA $g^{-1}$; 50 mA h $g^{-1}$ at 500 mA $g^{-1}$; 25 mA h $g^{-1}$ at 1000 mA $g^{-1}$; | 274 mA h $g^{-1}$ after 195 cycles at 20 mA $g^{-1}$, ~90.6%; | 83 | [14] |
| Rice husk | 1 M $NaClO_4$ in EC/DEC | 265 mA h $g^{-1}$ at 500 mA $g^{-1}$; 166 mA h $g^{-1}$ at 1000 mA $g^{-1}$; | 346 mA h $g^{-1}$ after 100 cycles at 25 mA $g^{-1}$, ~93%; | 66 | [15] |
| Sucrose | 0.8 M $NaPF_6$ in EC/DEC; 0.8 M $NaPF_6$ in DEGDME | 215/250 mA h $g^{-1}$ at 0.1 A $g^{-1}$; 100/220 mA h $g^{-1}$ at 0.5 A $g^{-1}$; 80/200 mA h $g^{-1}$ at 1.0 A $g^{-1}$; | 240 mA h $g^{-1}$ after 150 cycles at 50 mA $g^{-1}$, ~100%; 230 mA h $g^{-1}$ after 150 cycles at 50 mA $g^{-1}$, ~93.7%; | 70.9<br>83.8 | [16] |
| Lotus stems | 1 M $NaClO_4$ in EC/DEC | 351 mA h $g^{-1}$ at 40 mA $g^{-1}$; 290 mA h $g^{-1}$ at 100 mA $g^{-1}$; 240 mA h $g^{-1}$ at 200 mA $g^{-1}$; 150 mA h $g^{-1}$ at 500 mA $g^{-1}$; | 330 mA h $g^{-1}$ after 450 cycles at 100 mA $g^{-1}$, ~94%; | 70 | [17] |
| Poplar wood | 1 M $NaPF_6$ in EC/DMC | 310 mA h $g^{-1}$ at 60 mA $g^{-1}$; 290 mA h $g^{-1}$ at 150 mA $g^{-1}$; 180 mA h $g^{-1}$ at 300 mA $g^{-1}$; | 330 mA h $g^{-1}$ after 100 cycles at 30 mA $g^{-1}$; | 88.3 | [18] |
| Expanded HC | 1 M $NaClO_4$ PC, 5% FEC | 298.7 mA h $g^{-1}$ at 20 mA $g^{-1}$; 236.5 mA h $g^{-1}$ at 100 mA $g^{-1}$; 146.7 mA h $g^{-1}$ at 1000 mA $g^{-1}$; | 298 mA h $g^{-1}$ after 100 cycles at 100 mA $g^{-1}$, ~99%; 132 mA h $g^{-1}$ after 500 cycles at 500 mA $g^{-1}$, ~89.8%; | 67.3 | [19] |

**References:**

[1] P. Liu, Y. Li, Y. S. Hu, H. Li, L. Chen, X. Huang, *J. Mater. Chem. A* **2016**, *4*, 13046–13052.

[2] N. Sun, H. Liu, B. Xu, *J. Mater. Chem. A* **2015**, *3*, 20560–20566.

[3] F. Wu, M. Zhang, Y. Bai, X. Wang, R. Dong, C. Wu, *ACS Appl. Mater. Interfaces* **2019**, *11*, 12554–12561.

[4] F. Shen, H. Zhu, W. Luo, J. Wan, L. Zhou, J. Dai, B. Zhao, X. Han, K. Fu, L. Hu, *ACS Appl. Mater. Interfaces* **2015**, *7*, 23291–23296.

[5] Y. Bai, Y. Liu, Y. Li, L. Ling, F. Wu, C. Wu, *RSC Adv*., **2017**, *7*, 5519–5527.

[6] Z. Hong, Y. Zhen, Y. Ruan, M. Kang, K. Zhou, J. M. Zhang, Z. Huang, M. Wei, *Adv. Mater*., **2018**, *30*, 1802035.

[7] Z. Li, L. Ma, T. W. Surta, C. Bommier, Z. Jian, Z. Xing, W. F. Stickle, M. Dolgos, K. Amine, J. Lu,

T. Wu, X. Ji, *ACS Energy Lett*., **2016**, *1*, 395–401.

[8] Y. Li, Y. Yuan, Y. Bai, Y. Liu, Z. Wang, L. Li, F. Wu, K. Amine, C. Wu, J. Lu, *Adv. Energy Mater*., **2018**, *8*, 1702781.

[9] Y. He, P. Bai, S. Gao, Y. Xu, *ACS Appl. Mater. Interfaces* **2018**, *10*, 41380–41388.

[10] Y. E. Zhu, L. Yang, X. Zhou, F. Li, J. Wei, Z. Zhou, *J. Mater. Chem. A* **2017**, *5*, 9528–9532.

[11] P. Bai, Y. He, P. Xiong, X. Zhao, K. Xu, Y. Xu, *Energy Storage Mater.*, **2018**, *13*, 274.

[12] Y. Li, Y. S. Hu, M. M. Titirici, L. Chen, X. Huang, *Adv. Energy Mater.*, **2016**, *6*, 1600659.

[13] K. L. Hong, L. Qie, R. Zeng, Z. Q. Yi, W. Zhang, D. Wang, W. Yin, C. Wu, Q. J. Fan, W. X. Zhang, Y. H. Huang, *J. Mater. Chem. A* **2014**, *2*, 12733.

[14] Y. Li, S. Xu, X. Wu, J. Yu, Y. Wang, Y. S. Hu, H. Li, L. Chen, X. Huang, *J. Mater. Chem. A* **2015**, *3*, 71.

[15] W. Luo, C. Bommier, Z. Jian, X. Li, R. Carter, S. Vail, Y. Lu, J. J. Lee, X. Ji, *ACS Appl. Mater. Interfaces* **2015**, *7*, 2626.

[16] Q. Wang, X. Zhu, Y. Liu, Y. Fang, X. Zhou, J. Bao, *Carbon* **2018**, *127*, 658.

[17] N. Zhang, Q. Liu, W. Chen, M. Wan, X. Li, L. Wang, L. Xue, W. Zhang, *J. Power Sources* **2018**, *378*, 331.

[18] Y. Zheng, Y. Lu, X. Qi, Y. Wang, L. Mu, Y. Li, Q. Ma, J. Li, Y. S. Hu, *Energy Storage Mater.*, **2018**, *18*, 269.

[19] Z. Zhu, F. Liang, Z. Zhou, X. Zeng, D. Wang, P. Dong, J. Zhao, S. Sun, Y. Zhang, X. Li, *J. Mater. Chem. A* **2018**, *6*, 1513.